This is a repository copy of *Multi-dimensional photonic states from a quantum dot*.

White Rose Research Online URL for this paper:
http://eprints.whiterose.ac.uk/137720/

Version: Published Version

Article:
Lee, J.P., Bennett, A.J., Stevenson, R.M. et al. (4 more authors) (2018) Multi-dimensional photonic states from a quantum dot. Quantum Science and Technology, 3 (2).

https://doi.org/10.1088/2058-9565/aaa7b7

Reuse
This article is distributed under the terms of the Creative Commons Attribution (CC BY) licence. This licence allows you to distribute, remix, tweak, and build upon the work, even commercially, as long as you credit the authors for the original work. More information and the full terms of the licence here:
https://creativecommons.org/licenses/

Takedown
If you consider content in White Rose Research Online to be in breach of UK law, please notify us by emailing eprints@whiterose.ac.uk including the URL of the record and the reason for the withdrawal request.

eprints@whiterose.ac.uk
https://eprints.whiterose.ac.uk/

Quantum Science and Technology

PAPER • **OPEN ACCESS**

Multi-dimensional photonic states from a quantum dot

To cite this article: J P Lee *et al* 2018 *Quantum Sci. Technol.* **3** 024008

View the article online for updates and enhancements.

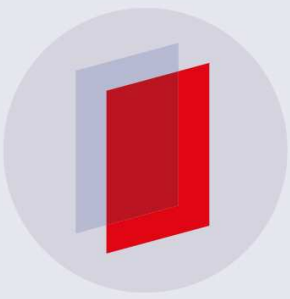

IOP ebooks™

Bringing you innovative digital publishing with leading voices to create your essential collection of books in STEM research.

Start exploring the collection - download the first chapter of every title for free.

This content was downloaded from IP address 143.167.29.212 on 25/10/2018 at 11:59

Quantum Science and Technology

PAPER

Multi-dimensional photonic states from a quantum dot

J P Lee[1,2], A J Bennett[1,4,5], R M Stevenson[1], D J P Ellis[1], I Farrer[3,6], D A Ritchie[3] and A J Shields[1]

[1] Toshiba Research Europe Limited, Cambridge Research Laboratory, 208 Science Park, Milton Road, Cambridge, CB4 0GZ, United Kingdom
[2] Engineering Department, University of Cambridge, 9 J. J. Thomson Avenue, Cambridge, CB3 0FA, United Kingdom
[3] Cavendish Laboratory, Cambridge University, J. J. Thomson Avenue, Cambridge, CB3 0HE, United Kingdom
[4] Current affiliation: Institute for Compound Semiconductors, Cardiff University, Queen's Buildings, 5 The Parade, Roath, Cardiff, CF24 3AA, United Kingdom.
[5] Author to whom any correspondence should be addressed.
[6] Current affiliation: Department of Electronic & Electrical Engineering, University of Sheffield, Mappin Street, Sheffield, S1 3JD, United Kingdom.

E-mail: BennettA19@cardiff.ac.uk

Keywords: quantum dots, Raman scattering, quantum information, quantum optics, photonics, cavity QED

OPEN ACCESS

RECEIVED
31 October 2017

REVISED
8 January 2018

ACCEPTED FOR PUBLICATION
15 January 2018

PUBLISHED
7 February 2018

Original content from this work may be used under the terms of the Creative Commons Attribution 3.0 licence.

Any further distribution of this work must maintain attribution to the author(s) and the title of the work, journal citation and DOI.

Abstract

Quantum states superposed across multiple particles or degrees of freedom offer an advantage in the development of quantum technologies. Creating these states deterministically and with high efficiency is an ongoing challenge. A promising approach is the repeated excitation of multi-level quantum emitters, which have been shown to naturally generate light with quantum statistics. Here we describe how to create one class of higher dimensional quantum state, a so called W-state, which is superposed across multiple time bins. We do this by repeated Raman scattering of photons from a charged quantum dot in a pillar microcavity. We show this method can be scaled to larger dimensions with no reduction in coherence or single-photon character. We explain how to extend this work to enable the deterministic creation of arbitrary time-bin encoded qudits.

1. Introduction

Photonic states with multiple components are a useful resource for secure quantum relays [1], measurement based quantum computers [2] and quantum enhanced sensors [3]. Many early demonstrations of these technologies have made use of the polarisation degree of freedom, which is simple to produce and manipulate but is limited to two dimensions [4]. The challenge of extending these quantum states to greater dimensions in a scalable way, through adding extra quantum bits or degrees of freedom, promises new functionality and greater resistance to errors. In some cases replacing the 'quantum bit' with a three dimensional qutrit or a d-dimensional qudit has clear advantages, for instance in quantum communication where the larger alphabet of characters allows transmission of more than one bit of classical information per photon [5]. Such higher dimensional states can be encoded in the photon path, orbital angular momentum [6], the radial degree of freedom [7], temporal modes [8], or perhaps most naturally in separate time bins [9, 10].

One interesting class of higher dimensional photonic state has the form

$$|W\rangle = \frac{|001\rangle + e^{-i\phi_1}|010\rangle + e^{-i\phi_2}|100\rangle}{\sqrt{3}}. \quad (1)$$

When $e^{-i\phi_1} = e^{-i\phi_2} = 1$, this is known as a W-state. In the case of a single-photon W-state, this can take the form of a single photon superposed across multiple modes. W-states have uses ranging from fundamental investigations of quantum mechanics to imaging and random number generation[11–14].

There are several approaches to realising higher dimensional photonic states. For example, it has been demonstrated that the widely studied parametric generation of entangled photon pairs can be extended to photon triplets [15]. It is also possible to fuse together [16] or entangle [17] smaller photonic states in a gate operation, but even for state-of-the-art technologies these approaches are probabilistic or have limited fidelities

© 2018 IOP Publishing Ltd

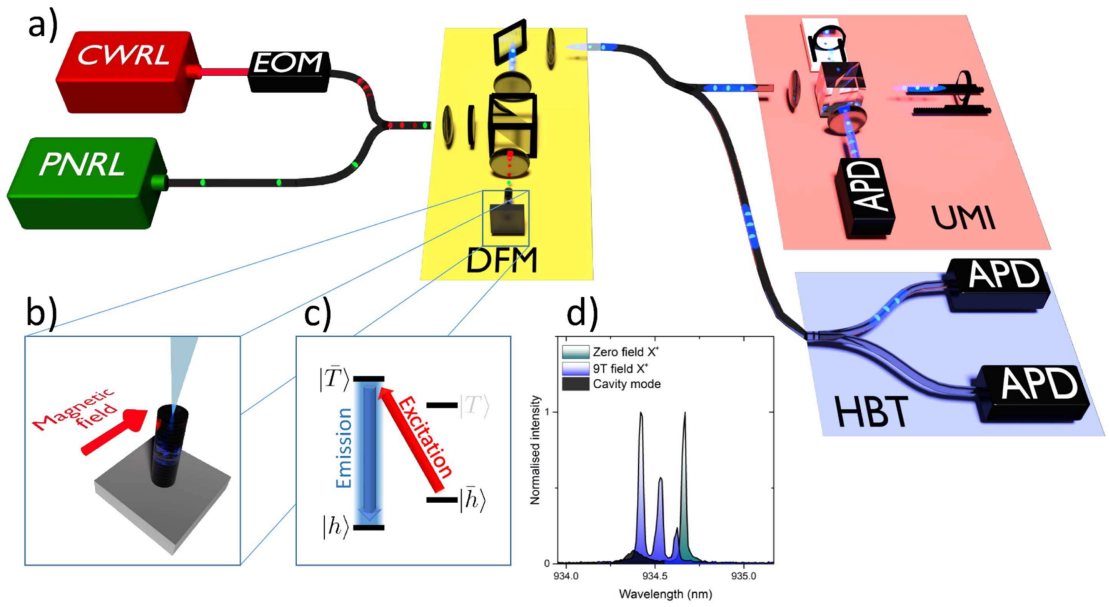

Figure 1. (a) An illustration of the experimental setup. (b) The QD-micropillar system is cooled in a cryostat to 5 K and placed in a Voigt geometry magnetic field. A pulsed non-resonant laser (PNRL) is used to apply short non-resonant pulses and a continuous-wave resonant laser (CWRL) is modulated using an electro-optic modulator (EOM) to create a series of pulses. The light is focused on the sample via a dark field microscope (DFM) that makes use of polarisation and spectral filtering to separate the output light emitted from the QD from the input laser light. The output light is then either directed into one of two detection setups. The output light can be directed into a Hanbury Brown and Twiss (HBT) setup consisting of a beam splitter and two avalanche photo-diodes (APDs). The output can also be directed into an unbalanced Michelson interferometer (UMI). (c) The energy level diagram shows the states and allowed transitions of a single-hole charged quantum dot in a Voigt field. The highest energy vertical transition is cavity enhanced (shown as blue) and the $|\bar{h}\rangle \rightarrow |\bar{T}\rangle$ transition is driven by the CWRL (shown as red). (d) The spectrum of the X^{+} transitions at zero magnetic field and the observed spectrum of the X^{+} transitions when the sample is placed in a 9 T Voigt geometry magnetic field with the shortest wavelength transition enhanced by the cavity mode. Note that the two diagonal transitions cannot be resolved by our spectrometer (resolution 30 μeV) and so appear as a single peak. The spectrum was produced using non-resonant light with a wavelength of 850 nm.

[18], which reduces the efficiency. An attractive option is to directly generate a complex photonic state from a single quantum emitter [19, 20], which in principle allows the deterministic generation of multi-qubit photonic states. In fact, it has been argued that creating entangled photonic states on demand would be the final enabling technology in the development of a photonic quantum computer [21, 22]. Trapped spins in quantum dots have been shown to be suitable multi-level emitters for this purpose [23, 24]. In addition, they have been used to demonstrate coherent spin manipulations [25], spin-photon entanglement [26, 27] and distant entanglement between two spins [28].

In this work, we use a cavity-enhanced Raman transition in a quantum dot (QD) to show enhanced spin preparation and then to sequentially generate time-bin-encoded single-photon W-states. Firstly, we demonstrate that a high Q-factor micropillar cavity allows us to observe cavity-stimulated Raman emission. We use this effect to perform spin state preparation [29] on a trapped hole spin over an order of magnitude faster than in the non-cavity-enhanced case. We then demonstrate our interferometer free scheme for W-state generation. The scheme can be trivially scaled to higher dimensions—we show this by producing photons superposed across up to four time bins. Finally, we explain how the techniques demonstrated in this work could allow the deterministic generation of arbitrary single-photon time bin encoded states. We anticipate that this capability will prove useful for single-mode quantum computation [30] and for maximising the key rates of QKD protocols over long distances [31–33].

2. Methods and results

2.1. Cavity-enhanced spin preparation

We perform our experiments using a single-hole charged quantum dot in a micropillar cavity (figure 1(b)), a system which has been shown to be a good source of indistinguishable photons [34]. The device we use is nominally undoped, emission from the positively charged state can be activated by weak non-resonant light at a wavelength of 850 nm [34]. Applying a Voigt geometry magnetic field results in a double-Λ system. The magnetic field and temperature are tuned so that a single vertical transition is cavity enhanced (figure 1(c)). The states of the system are aligned parallel/anti-parallel to the magnetic field. We label the hole spin states, $|h\rangle/|\bar{h}\rangle = \frac{|\Uparrow\rangle \pm |\Downarrow\rangle}{\sqrt{2}}$ and the trion states as $|T\rangle/|\bar{T}\rangle = \frac{|\Uparrow\downarrow\uparrow\rangle \pm |\Uparrow\Downarrow\uparrow\rangle}{\sqrt{2}}$.

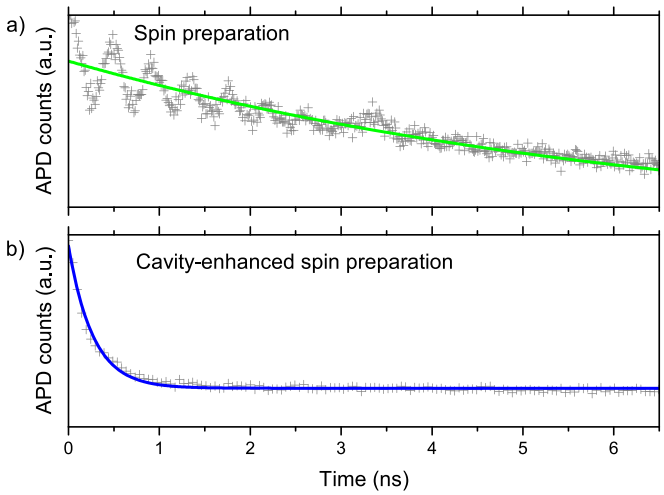

Figure 2. (a) A graph showing the decrease in Avalanche Photo-diode (APD) counts over time due to spin pumping of trapped spin in a QD in a Voigt geometry magnetic field with no Purcell enhancement. The sinusoidal oscillations visible in the raw data are a result of Rabi oscillations between the levels driven by the resonant laser. The underlying exponential decay time (fitted green line) is 6.71 ± 0.55 ns. (b) A graph showing the decrease in photon emission probability over time due to spin pumping in our Purcell enhanced system. The fitted exponential decay (blue line) has a decay time of 270 ± 6 ps.

In order to maximise the number of operations that can be performed on a spin per unit time, it is desirable to perform spin state preparation as rapidly as possible. In the Voigt configuration the spin preparation typically takes several nanoseconds [35].

In our experiments we use a micropillar cavity to decrease the spin preparation time. In the Raman process a photon from the laser is scattered resulting in a photon that we detect at the energy of the $|\bar{T}\rangle \rightarrow |h\rangle$ transition. Driving the $|\bar{h}\rangle \rightarrow |\bar{T}\rangle$ transition we observe cavity-stimulated Raman emission [36]. This increases the speed of spin preparation because the system is more likely to decay via the enhanced vertical transition than the non-enhanced diagonal transition. As a result we can perform spin preparation in 270 ± 6 ps—over an order of magnitude faster than is typically seen for similar non-cavity-enhanced systems (figure 2). We note that there is a continued background emission in figure 2(b) once spin preparation has occurred—we attribute the to the similarity in energy of the diagonal transitions in this quantum dot. The resonant laser may weakly drive the $|h\rangle \rightarrow |T\rangle$ transition as well as the intended transition, lowering the spin preparation fidelity in this case. Higher magnetic fields or a quantum dot with a different combination of electron and whole g-factors could remove this effect.

We also note that the selective enhancement of one transition of the lambda system means that it could function as a cycling transition to be used for spin readout [37, 38]. The ability to perform rapid spin preparation and reliable spin readout in the Voigt geometry will help make trapped spins in quantum dots appealing candidates for stationary qubits and light matter interfaces. Our pillar microcavity has negligible polarisation splitting and although it enhances transitions resonant with the mode, it does not suppress detuned transitions. Non-resonant excitation of the 4 level system in figure 1(d) results in equal populations in states $|\bar{T}\rangle$ and $|T\rangle$, which decay via 4 unequal decay channels, which we collect with unequal efficiencies. The ratio of the area of the longest and shortest wavelength peaks in the spectrum of the X^- transitions at 9 T (figure 1(d)) suggest the cavity-enhanced decay is a factor of ~4.1 faster than the non-enhanced case. Similarly, comparing the spin preparation time recorded by driving the $|\bar{h}\rangle \rightarrow |\bar{T}\rangle$ and measuring light from the $|\bar{T}\rangle \rightarrow |h\rangle$ (cavity-enhanced preparation) and the spin preparation time recorded by driving the $|h\rangle \rightarrow |\bar{T}\rangle$ and measuring light from the $|\bar{T}\rangle \rightarrow |\bar{h}\rangle$ gives us a ratio of ~4.8.

The coherence time of the Raman scattered photons is determined by the coherence of the long lived ground state hole spin and the laser rather than the shorter coherence time of the exciton [39, 40]. This means that the coherence of the photon state is in part inherited from the highly coherent laser light. A further useful property of Raman emission is that the wavelength of the emitted photons can be tuned by tuning the wavelength of the excitation laser [36, 41]. In our system we observe a tuning range of over 65 μeV. This would allow for the generation of indistinguishable photons from different sources—a key requirement for several quantum photonic technologies [16, 42].

2.2. The sequential generation of time-bin encoded W-States

Here we implement a scheme for the generation of a single-photon W-state. W-states are of particular interest as they represent one of two types of maximally entangled tripartite states and maintain their entanglement in the presence of dissipation [43]. The concept can be generalized to include W-states with more than three qubits.

We use a series of weak resonant pulses (shown in figure 3(a)) to drive the $|\bar{h}\rangle \rightarrow |\bar{T}\rangle$ transition (shown as the red arrow in figure 1(c)). The power of these pulses is tuned so that they each have the same probability of driving

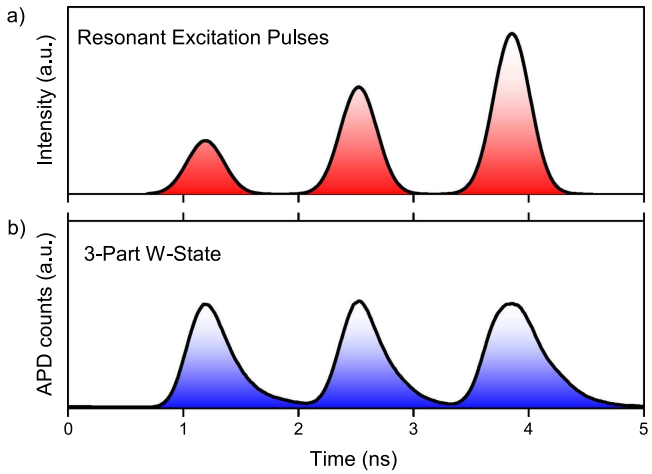

Figure 3. (a) An illustration of the pulse sequence used to create a 3 qubit single-photon W-State. The series of three pulses is used to drive the Raman transition and create a W-state photon. (b) A time resolved measurement of the collected light. Spectral filtering ensures that the collected light is at the wavelength of the cavity-enhanced transition.

the transition and generating a photon. When the $|\bar{h}\rangle \rightarrow |\bar{T}\rangle$ transition is driven, the system preferentially decays vertically (shown as the blue transition in figure 1(c)). The emitted photon has an equal probability of being measured in each time bin (figure 3(b)). The light produced by this mechanism is emitted as single quanta because the detection of a photon at the wavelength of the enhanced transition heralds the preparation of the hole spin in the $|h\rangle$ state. Once in the $|h\rangle$ state the system cannot be re-excited by the laser driving the $|\bar{h}\rangle \rightarrow |\bar{T}\rangle$ transition until a spin-flip occurs. Spin-flips typically take three orders of magnitude longer than the W-state generation process and so are not of concern here [44]. In contrast, the single-photon emission that is usually observed from quantum dots relies on the spontaneous decay time of a transition being greater than the applied pulse length [45].

The setup for our scheme is shown in figure 1(a). A non-resonant pulse ensures that there is a non-zero population in the $|\bar{h}\rangle$ state. Then resonant pulses produced using a continuous-wave laser and an electro-optic modulator (EOM) are used to drive the Raman transition.

First, we use a single resonant pulse and second-order correlation function measurement to demonstrate that the system can act as a single-photon source. figure 4(a) shows a time resolved measurement of the output photons and figure 4(e) shows the second-order correlation function measurement. The low $g^{(2)}(0) \approx 0.02$ indicates that the output light is primarily composed of single photons.

We then use a two pulse sequence to create a photon superposed across two time bins (figure 4(b)). Extending this to a three pulse sequence we generate a single-photon three-part W-state (figure 4(c)). Finally, we use a four pulse sequence to create a four part W-state and demonstrate the scalability of our scheme (figure 4(d)). The output light for all of the pulse sequences have a greatly reduced peak in the second-order correlation function at $\tau = 0$, indicating that the output is dominated by single-photon emission (figures 4(e)–(h)). We work in the low efficiency regime using a resonant laser power well below saturation. This means that the $|\bar{h}\rangle$ population is not completely depleted by the final pulse of a pulse sequence, allowing us to add additional pulses to the end of the sequence to increase the dimensionality of the photonic state without requiring the recalibration of each pulse power.

We also observe anti-bunching over tens of nanoseconds; the peaks at $\tau = \pm 12.5$ ns are lower than the other peaks away from $\tau = 0$. This indicates that the non-resonant pulse does not completely randomise the hole spin state meaning that a photon is less likely to be generated if a photon has been produced during the preceding excitation sequence. This effect could be removed by deterministic preparation of the spin in the $|\bar{h}\rangle$ state prior to the incidence of the resonant laser pulses.

Finally, we probe the coherence between neighbouring time bins of the three-part W-state by time resolving the output of an unbalanced Michelson interferometer. This measurement shows that the photons are in a coherent superposition between different time bins and not simply emitted into one time bin or another probabilistically. The long arm of the interferometer delays the light by one time-bin relative to the short arm (figures 4(i) and (j)). This means that we expect to see interference between time-bin 1 and time-bin 2, and between time-bin 2 and time-bin 3 of a single 3-time-bin photon [46].

By varying the phase difference between the two arms we observe interference between the overlapping time bins (figure 4(k)). The interference measurements were also performed for the 2 and 4 part W-states; the visibilities obtained by fitting a sinusoidal function to the measured intensities of the overlapping time bins as a

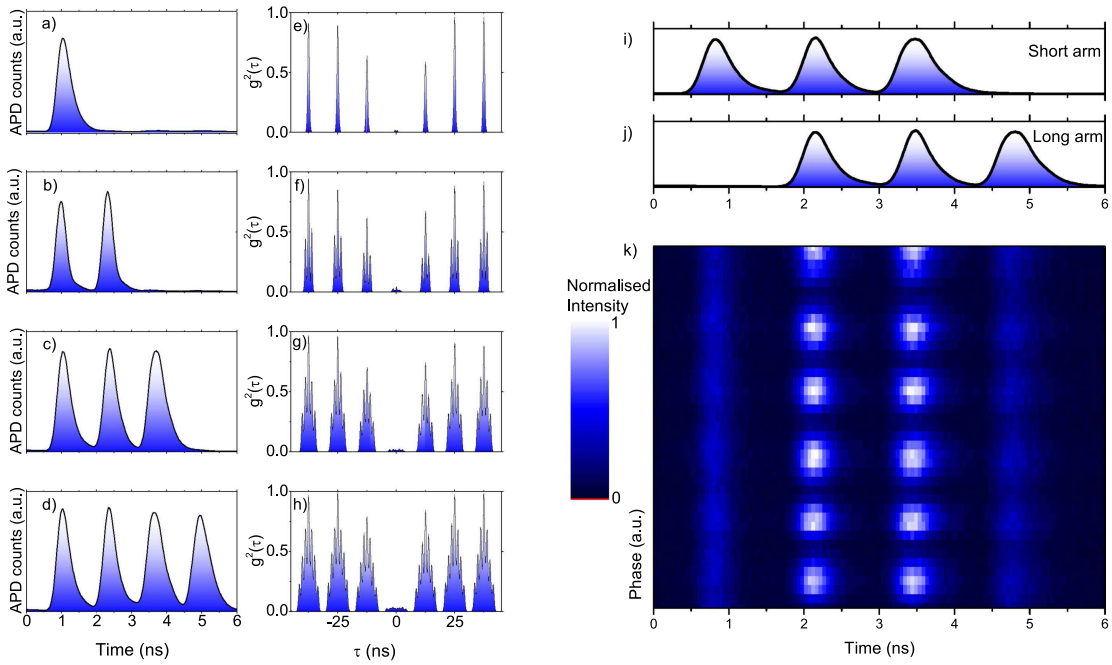

Figure 4. (a–d) Time resolved measurements of the produced photons superposed across 1, 2, 3 and 4 time-bins. (e–h) Second-order correlation function measurements on the produced W-state photons confirm their single-photon nature. (i, j) Time resolved measurements showing the single-time-bin offset introduced by the difference in the short and long paths of the unbalanced Michelson interferometer. (k) A time resolved interference measurement showing interference between neighbouring time bins of a single photon superposed across three time bins.

Table 1. Coherent single-photon states.

# Time bins	$g^{(2)}(0)$	Visibility
1	0.0233 ± 0.0009	—
2	0.0463 ± 0.0012	65.6 ± 4.3%
3	0.0309 ± 0.0004	69.6 ± 5.4%
4	0.0577 ± 0.0004	67.7 ± 5.7%

function of phase are shown in table 1. The phase of the photon is determined by the phase of the laser and the phase of the hole spin. We attribute the deviation from perfect interference visibility to the non-zero probability of a decay along the $|\bar{T}\rangle \rightarrow |\bar{h}\rangle$ transition and the decoherence of the hole spin.

2.3. Proposal for the deterministic generation of single-photon W-States

As quantum dots in high Q cavities can act as deterministic photon sources [47], we propose an extension to our scheme to generate generate W-States deterministically. We assume that a future experiment will be performed with a quantum dot deterministically charged with a single charge, either an electron or a hole, which could be introduced by tunneling in an appropriately biased diode structure [48] or a deliberately doped dot [49]. Our proposal is as follows:

1. Ensure that the system in the state $|\bar{h}\rangle$ by first preparing the $|h\rangle$ state as demonstrated earlier, then using an off-resonant pulse to perform a π-rotation of the hole spin [25, 37, 50].
2. Apply a $\frac{\pi}{3}$ pulse to the diagonal transition indicated in figure 2(a). The resulting Raman emission leaves us with the state $\sqrt{\frac{2}{3}}|\bar{h}\rangle|0_{\tau=1}\rangle + \frac{1}{\sqrt{3}}|h\rangle|1_{\tau=1}\rangle$, where $|0_{\tau=1}\rangle$ ($|1_{\tau=1}\rangle$) indicates the absence (presence) of a photon in time-bin 1.
3. A $\frac{\pi}{2}$ pulse leaves us with the state $\frac{1}{\sqrt{3}}|\bar{h}\rangle|0_{\tau=2}0_{\tau=1}\rangle + \frac{1}{\sqrt{3}}|h\rangle|1_{\tau=2}0_{\tau=1}\rangle + \frac{1}{\sqrt{3}}|h\rangle|0_{\tau=2}1_{\tau=1}\rangle$.
4. A final π pulse leaves us with the state $\frac{1}{\sqrt{3}}|h\rangle|1_{\tau=3}0_{\tau=2}0_{\tau=1}\rangle + \frac{1}{\sqrt{3}}|h\rangle|0_{\tau=3}1_{\tau=2}0_{\tau=1}\rangle + \frac{1}{\sqrt{3}}|h\rangle|0_{\tau=3}0_{\tau=2}1_{\tau=1}\rangle$.

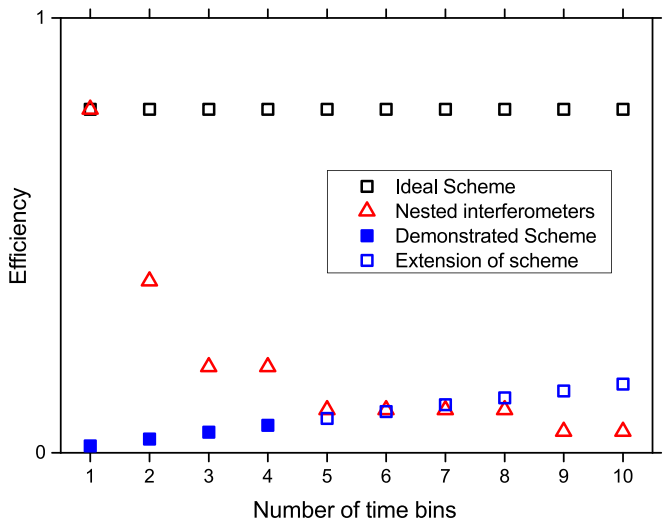

Figure 5. A graph showing the estimated efficiencies for several different approaches to generating multi-qubit time-bin-encoded single-photon states. The starting efficiency is the extraction efficiency of photons from a QD embedded in a micropillar cavity [53]. For the ideal scheme (black squares), we assume deterministic hole injection and preparation and no diagonal decay. For the nested interferometer scheme (red triangles), we assume the that mirrors and beam splitters are ideal and that only 50:50 beam splitters are used. For the demonstrated scheme (blue squares), we assume that the non-resonant pulse injects a hole spin with a 50% success probability (not measured for this sample, but this is within the range seen in similar samples) and that we have a 50% probability of any spin present being in the $|\bar{h}\rangle$ state. We also assume that the branching ratio between the bright and dark transitions is 5 and that the probability of the first pulse generating a photon is 0.1. The fully shaded blue squares indicate the states produced during this work.

Ignoring the hole state and considering the state of the photon in isolation it is clear that this gives us with a photon in the state $\frac{1}{\sqrt{3}}(|001\rangle + |010\rangle + |100\rangle)$ — a single-photon W-state. For the success of this scheme, future work must investigate whether the use of a sequence of Raman pulses that result in a deterministic photon generation are going to reduce the coherence of the single, multi-time-bin Raman photon or whether the improved coherence properties of the emitted light due to the Purcell enhancement (discussed in [40] and [34]) will be enough to counter any detrimental effects of a higher laser power.

2.4. Additional experimental details

The experiments were performed using an InAs quantum dot in a GaAs/AlGaAs micropillar cavity with a Q-factor of ~7500. The dot-cavity system was cooled to 5 K and placed in a 9 T Voigt geometry magnetic field. The resonant pulses are generated using a continuous-wave diode laser at ~940 nm and electro-optic modulator. The resonant pulses are separated from the emitted light by both polarisation and spectral filtering. To record the HBT measurements we time-tag each photon, this allows us to remove the effect of photons generated from the non-resonant pulses on the correlation measurements through temporal filtering. The unbalanced Michelson interferometer used was kept at a constant temperature in order to minimise drift.

3. Discussion and conclusions

We have described how to directly generate higher dimensional time-bin-encoded quantum states without an interferometer but with sub-Poissonian statistics using Raman scattering from a single quantum emitter. The use of an EOM in this scheme allows us to make use of flexible electronic triggering [51] to determine the probability amplitudes of the photon for each time bin.

A phase modulator could be used to control the relative phase of the laser between two resonant pulses to create a qubit suitable for time-bin-encoded quantum key distribution [52]. This phase modulation could also be achieved by using a detuned pulse to rotate the hole spin about the z-axis of the Bloch sphere [28]. In combination with the demonstrated ability to control the amplitude of each time bin, this would allow the creation of arbitrary single-photon time-bin-encoded states without the use of nested interferometers, which have efficiencies that decrease exponentially with the number of beam splitters. Figure 5 shows how the efficiencies for our scheme (both the implemented and ideal versions) compare with the efficiency of using a nested interferometer setup. We note that using weak pulses in our implementation results in the probability of generating a photon increasing with the number of time bins. The estimates shown here indicate that although the experiments demonstrated so far are less efficient than simply using nested interferometers, we expect our

scheme to become more efficient when states with 8 or more time bins are considered. In addition, the ideal scheme would be more efficient than using nested interferometers for any time-bin-encoded state.

Using continuously varied excitation rather than pulsed excitation would allow the generation of arbitrarily shaped photons [54]. This, in addition to phase modulation would enable to encode quantum information in the temporal mode of a photon [55]. In combination with the wavelength tuning made possible by the cavity-enhanced Raman emission process this will allow the generation of photons from QD sources that are indistinguishable from photons from other light sources such as lasers and trapped atoms. We expect our results to pave the way for solid state sources of on-demand photonic qubits and efficient interfaces between quantum dots and other quantum optical systems.

Data access

The experimental data used to produce the figures in this paper is publicly available at https://doi.org/10.17863/CAM.17218.

Acknowledgments

The authors acknowledge funding from the EPSRC for MBE system used in the growth of the micropillar cavity. J L gratefully acknowledges financial support from the EPSRC CDT in Photonic Systems Development and Toshiba Research Europe Ltd.

ORCID iDs

J P Lee https://orcid.org/0000-0001-5653-7331

References

[1] Collins D, Gisin N and De Riedmatten H 2005 *J. Mod. Opt.* **52** 735
[2] Raussendorf R, Browne D E and Briegel H J 2003 *Phys. Rev.* A **68** 022312
[3] Giovannetti V, Lloyd S and Maccone L 2004 *Science* **306** 1330
[4] Nagali E, Sciarrino F, De Martini F, Marrucci L, Piccirillo B, Karimi E and Santamato E 2009 *Phys. Rev. Lett.* **103** 013601
[5] Bechmann-Pasquinucci H and Tittel W 2000 *Phys. Rev.* A **61** 062308
[6] Mair A, Vaziri A, Weihs G and Zeilinger A 2001 *Nature* **412** 313
[7] Karimi E, Giovannini D, Bolduc E, Bent N, Miatto F M, Padgett M J and Boyd R W 2014 *Phys. Rev.* A **89** 013829
[8] Polycarpou C, Cassemiro K N, Venturi G, Zavatta A and Bellini M 2012 *Phys. Rev. Lett.* **109** 053602
[9] Brendel J, Gisin N, Tittel W and Zbinden H 1999 *Phys. Rev. Lett.* **82** 2594
[10] Jayakumar H, Predojević A, Kauten T, Huber T, Solomon G S and Weihs G 2014 *Nat. Commun.* **5** 4251
[11] Chaves R and Brask J B 2011 *Phys. Rev.* A **84** 062110
[12] Heaney L, Cabello A, Santos M F and Vedral V 2011 *New J. Phys.* **13** 053054
[13] Gottesman D, Jennewein T and Croke S 2012 *Phys. Rev. Lett.* **109** 070503
[14] Gräfe M, Heilmann R, Perez-Leija A, Keil R, Dreisow F, Heinrich M, Moya-Cessa H, Nolte S, Christodoulides D N and Szameit A 2014 *Nat. Photon.* **8** 791
[15] Hübel H, Hamel D R, Fedrizzi A, Ramelow S, Resch K J and Jennewein T 2010 *Nature* **466** 601
[16] Browne D E and Rudolph T 2005 *Phys. Rev. Lett.* **95** 010501
[17] O'Brien J L, Pryde G J, White A G, Ralph T C and Branning D 2003 *Nature* **426** 264
[18] Hacker B, Welte S, Rempe G and Ritter S 2016 *Nature* **536** 193
[19] Schön C, Solano E, Verstraete F, Cirac J I and Wolf M M 2005 *Phys. Rev. Lett.* **95** 110503
[20] Schön C, Hammerer K, Wolf M M, Cirac J I and Solano E 2007 *Phys. Rev.* A **75** 032311
[21] Gimeno-Segovia M, Shadbolt P, Browne D E and Rudolph T 2015 *Phys. Rev. Lett.* **115** 020502
[22] Rudolph T 2017 *APL Photonics* **2** 030901
[23] Lindner N H and Rudolph T 2009 *Phys. Rev. Lett.* **103** 113602
[24] Schwartz I, Cogan D, Schmidgall E R, Don Y, Gantz L, Kenneth O, Lindner N H and Gershoni D 2016 *Science* **354** 434–7
[25] Press D, Ladd T D, Zhang B and Yamamoto Y 2008 *Nature* **456** 218
[26] De Greve K *et al* 2012 *Nature* **491** 421
[27] Gao W B, Fallahi P, Togan E, Miguel-Sanchez J and Imamoglu A 2012 *Nature* **491** 426
[28] Delteil A, Sun Z, Gao W-B, Togan E, Faelt S and Imamoglu A 2015 *Nat. Phys.* **12** 218–23
[29] Atatüre M, Dreiser J, Badolato A, Högele A, Karrai K and Imamoglu A 2006 *Science* **312** 551
[30] Humphreys P C, Metcalf B J, Spring J B, Moore M, Jin X-M, Barbieri M, Kolthammer W S and Walmsley I A 2013 *Phys. Rev. Lett.* **111** 150501
[31] Zhong T *et al* 2015 *New J. Phys.* **17** 022002
[32] Sasaki T, Yamamoto Y and Koashi M 2014 *Nature* **509** 475
[33] Takesue H, Sasaki T, Tamaki K and Koashi M 2015 *Nat. Photon.* **9** 827–31
[34] Bennett A J, Lee J P, Ellis D J P, Meany T, Murray E, Floether F F, Griffths J P, Farrer I, Ritchie D A and Shields A J 2016 *Science Advances* **2** e1501256
[35] Emary C, Xu X, Steel D G, Saikin S and Sham L J 2007 *Phys. Rev. Lett.* **98** 047401

[36] Sweeney T M, Carter S G, Bracker A S, Kim M, Kim C S, Yang L, Vora P M, Brereton P G, Cleveland E R and Gammon D 2014 *Nat. Photon.* **8** 442–7
[37] Carter S G, Sweeney T M, Kim M, Kim C S, Solenov D, Economou S E, Reinecke T L, Yang L, Bracker A S and Gammon D 2013 *Nat. Photon.* **7** 329
[38] Sun S and Waks E 2016 *Phys. Rev.* A **94** 012307
[39] Fernandez G, Volz T, Desbuquois R, Badolato A and Imamoglu A 2009 *Phys. Rev. Lett.* **103** 087406
[40] Sun Z, Delteil A, Faelt S and Imamoğlu A 2016 *Phys. Rev.* B **93** 241302
[41] He Y *et al* 2013 *Phys. Rev. Lett.* **111** 237403
[42] Knill E, Laflamme R and Milburn G J 2001 *Nature* **409** 46
[43] Dür W, Vidal G and Cirac J I 2000 *Phys. Rev.* A **62** 062314
[44] Heiss D, Schaeck S, Huebl H, Bichler M, Abstreiter G, Finley J, Bulaev D and Loss D 2007 *Phys. Rev.* B **76** 241306
[45] Hours J, Varoutsis S, Gallart M, Bloch J, Robert-Philip I, Cavanna A, Abram I, Laruelle F and Gérard J M 2003 *Appl. Phys. Lett.* **82** 2206
[46] Sinha U, Couteau C, Jennewein T, Laflamme R and Weihs G 2010 *Science* **329** 418
[47] Nowak A *et al* 2014 *Nat. Commun.* **5** 3240
[48] Pinotsi D, Fallahi P, Miguel-Sanchez J and Imamoglu A 2011 *IEEE J. Quantum Electron.* **47** 1371
[49] Press D, De Greve K, McMahon P L, Ladd T D, Friess B, Schneider C, Kamp M, Höfling S, Forchel A and Yamamoto Y 2010 *Nat. Photon.* **4** 367
[50] Sun S, Kim H, Solomon G S and Waks E 2016 *Nat. Nanotechnol.* **11** 539
[51] Dada A C, Santana T S, Malein R N E, Koutroumanis A, Ma Y, Zajac J M, Lim J Y, Song J D and Gerardot B D 2016 *Optica* **3** 493
[52] Nisbet-Jones P B R, Dilley J, Holleczek A, Barter O and Kuhn A 2013 *New J. Phys.* **15** 053007
[53] Gazzano O, De Vasconcellos S M, Arnold C, Nowak A, Galopin E, Sagnes I, Lanco L, Lemaî A and Senellart P 2013 *Nat. Commun.* **4** 1425
[54] Nisbet-Jones P B R, Dilley J, Ljunggren D and Kuhn A 2011 *New J. Phys.* **13** 103036
[55] Brecht B, Reddy D V, Silberhorn C and Raymer M G 2016 *Phys. Rev.* X **6** 019901